OPEN ACCESS Freely available online

PLoS one

Kinin B_1 Receptor Enhances the Oxidative Stress in a Rat Model of Insulin Resistance: Outcome in Hypertension, Allodynia and Metabolic Complications

Jenny Pena Dias[1], Sébastien Talbot[1], Jacques Sénécal[1], Pierre Carayon[2], Réjean Couture[1]*

1 Department of Physiology, Faculty of Medicine, Université de Montréal, Montréal, Québec, Canada, **2** Sanofi-Aventis R&D, Montpellier, France

Abstract

Background: Kinin B_1 receptor (B_1R) is induced by the oxidative stress in models of diabetes mellitus. This study aims at determining whether B_1R activation could perpetuate the oxidative stress which leads to diabetic complications.

Methods and Findings: Young Sprague-Dawley rats were fed with 10% D-Glucose or tap water (controls) for 8–12 weeks. A selective B_1R antagonist (SSR240612) was administered acutely (3–30 mg/kg) or daily for a period of 7 days (10 mg/kg) and the impact was measured on systolic blood pressure, allodynia, protein and/or mRNA B_1R expression, aortic superoxide anion ($O_2^{\bullet-}$) production and expression of superoxide dismutase (MnSOD) and catalase. SSR240612 reduced dose-dependently (3–30 mg/kg) high blood pressure in 12-week glucose-fed rats, but had no effect in controls. Eight-week glucose-fed rats exhibited insulin resistance (HOMA index), hypertension, tactile and cold allodynia and significant increases of plasma levels of glucose and insulin. This was associated with higher aortic levels of $O_2^{\bullet-}$, NADPH oxidase activity, MnSOD and catalase expression. All these abnormalities including B_1R overexpression (spinal cord, aorta, liver and gastrocnemius muscle) were normalized by the prolonged treatment with SSR240612. The production of $O_2^{\bullet-}$ in the aorta of glucose-fed rats was also measured in the presence and absence of inhibitors (10–100 μM) of NADPH oxidase (apocynin), xanthine oxidase (allopurinol) or nitric oxide synthase (L-NAME) with and without Sar[D-Phe^8]des-Arg^9-BK (20 μM; B_1R agonist). Data show that the greater aortic $O_2^{\bullet-}$ production induced by the B_1R agonist was blocked only by apocynin.

Conclusions: Activation of kinin B_1R increased $O_2^{\bullet-}$ through the activation of NADPH oxidase in the vasculature. Prolonged blockade of B_1R restored cardiovascular, sensory and metabolic abnormalities by reducing oxidative stress and B_1R gene expression in this model.

Citation: Dias JP, Talbot S, Sénécal J, Carayon P, Couture R (2010) Kinin B_1 Receptor Enhances the Oxidative Stress in a Rat Model of Insulin Resistance: Outcome in Hypertension, Allodynia and Metabolic Complications. PLoS ONE 5(9): e12622. doi:10.1371/journal.pone.0012622

Editor: Krisztian Stadler, Louisiana State University, United States of America

Received June 4, 2010; **Accepted** August 12, 2010; **Published** September 7, 2010

Funding: This work was funded by Grants-in-Aid from the Canadian Diabetes Association (OG-3-07-2428) and the Canadian Institutes of Health Research (MOP-79471). Studentships Awards were obtained from the Canadian Diabetes Association (JPD), the Fonds de la Recherche en Santé du Québec (JPD, ST) and the Canadian Institutes of Health Research (JPD). Dr Pierre Carayon at Sanofi-Aventis R&D provided SSR240612 and approved the submission of the article with intellectual contribution. The funders had no role in study design, data collection and analysis, decision to publish, or preparation of the manuscript.

Competing Interests: Dr P. Carayon from Sanofi-Aventis R&D and Dr R. Couture from Université de Montréal hereby declare a duality of interest in view of their holding a patent made available to public in 2008 for the use of a non-peptide kinin B1 receptor antagonist in the treatment of hypertension (Publication No. 2916352). This does not alter adherence of these authors to all the PLoS ONE policies on sharing data and materials, as detailed online in the guide for authors. The other authors have nothing to disclose.

* E-mail: rejean.couture@umontreal.ca

Introduction

Recent evidence suggests a link between insulin resistance, oxidative stress, pain polyneuropathy and the overexpression of kinin B_1 receptor [1,2,3]. Kinins are vasoactive peptides and pro-inflammatory pain mediators which act through the activation of two G-protein-coupled receptors (R), named B_1 and B_2. While the B_1R has a low level of expression in healthy subjects, it is induced and overexpressed after exposure to pro-inflammatory cytokines, bacterial endotoxins and hyperglycaemia-induced oxidative stress [4,5]. Bradykinin (BK) and Lys-BK are the natural agonists for the constitutive B_2R, while the kininase I metabolites des-Arg^9-BK and Lys-des-Arg^9-BK are the selective agonists for the B_1R [6].

Autoradiographic and molecular studies showed an increased density of B_1R binding sites and mRNA in the brain, spinal cord and peripheral tissues of rats treated with D-Glucose (10% in drinking water) for a period of 4 and 12 weeks [2,3,7]. Glucose-fed rats displayed higher plasma levels of glucose and insulin, insulin resistance, arterial hypertension, enhanced production of superoxide anion ($O_2^{\bullet-}$) in the heart and aorta [8,9,10] and pain polyneuropathy as assessed by the presence of tactile and cold allodynia [1,2,3]. Recently, we reported that all these abnormalities including B_1R overexpression were reduced with a diet containing alpha-lipoic acid or N-Acetyl-L-Cysteine, two potent antioxidants [2,3], supporting a link between the upregulation of B_1R, diabetic complications and the oxidative stress. An acute treatment with B_1R antagonists (LF22-0542, SSR240612 and R-715) reversed tactile and cold allodynia in high glucose feeding [1,2]. However, only the brain penetrant B_1R antagonist (LF22-0542) and not the peripherally acting R-715 decreased high systolic blood pressure in glucose-fed rats [2].

The present study was undertaken to determine the beneficial effect of a prolonged treatment (1 week) with the centrally and peripherally acting B_1R antagonist SSR240612 on the main features and complications of diabetes in high glucose feeding. It is hypothesised that activation of B_1R increases oxidative stress (aortic $O_2^{\bullet-}$) and that its prolonged inhibition reverses oxidative stress and the subsequent upregulation of B_1R which is responsible for arterial hypertension and pain polyneuropathy. The source of $O_2^{\bullet-}$ was identified with the use of specific inhibitors of oxidative enzymes. The status of the antioxidant defence was determined by measuring the vascular expression of two selected antioxidant enzymes, superoxide dismutase (MnSOD) and catalase. MnSOD metabolises $O_2^{\bullet-}$ to hydrogen peroxide which is converted to water by catalase. The data highlight a detrimental role for B_1R in diabetes through a mechanism involving the oxidative stress and NADPH oxidase.

Materials and Methods

Animals and Procedures

Young male Sprague-Dawley rats (24–28 days old weighting 50–75 g, Charles River Laboratories, St-Constant, Quebec, Canada) were housed two per cage, under controlled conditions of temperature (22°C) and humidity (43%), on a 12-hour light-dark cycle and allowed free access to normal chow diet and tap water (control rats) or 10% D-glucose in the drinking water during 8 or 12 weeks for chronic and acute studies, respectively All research procedures and the care of the animals were in compliance with the guiding principles for animal experimentation as enunciated by the Canadian Council on Animal Care and were approved by the Animal Care Committee of our University (CDEA approval ID: 09-066).

Acute effect of SSR240612 on blood pressure

A first series of experiments was performed in 12-week glucose-fed rats to assess the acute effects of several doses of SSR240612 on systolic blood pressure in order to select the optimal dose for chronic experiment. SSR240612 was administered by gavage at doses of 3, 10 and 30 mg/kg and effects were measured up to 48 h post-administration in unanaesthetized rats. At the end of this protocol, rats were euthanized by CO_2 inhalation. Doses were selected on the basis of previous studies performed in various in vivo models of inflammation, pain and diabetes in rats and mice [11,12,13]. Moreover, these doses of SSR240612 were found appropriate to block acutely allodynia in the model of glucose-fed rats [1].

Chronic effect of SSR240612 on blood pressure, allodynia and other parameters

These studies were carried out in 4 groups of 8-week glucose feeding and control rats (diabetic and control ± vehicle, diabetic and control ± SSR240612). The dose of 10 mg/kg SSR240612 was selected for the chronic study on the basis of the dose-response curve constructed on blood pressure (present study) and allodynia [1]. This dose was administered by gavage once a day in the morning for one week in control rats and in rats fed with D-Glucose. Thus, effects of 10 mg/kg of SSR240612 were determined on allodynia and arterial hypertension at 0 h, 3 h, 6 h, 24 h, 48 h, 72 h, 96 h, 120 h, 144 h and 168 h post-gavage. On day 7, overnight-fasted rats were anaesthetized and then euthanized by CO_2 inhalation, 3 h after the last treatment with SSR240612, to collect tissues and blood samples for biochemical and molecular studies.

Measurement of plasma glucose, insulin and insulin resistance

At the end of protocol, overnight-fasted rats were slightly anaesthetized with CO_2 inhalation and blood was rapidly collected from sectioned carotid arteries and immediately transferred into a chilled tube of 6 ml containing 10.8 mg EDTA. The plasma was obtained by centrifugation and kept frozen at −20°C for the later measurement of glucose with a glucometer Accu-Chek (Roche Diagnostics Inc, Laval, Quebec, Canada) and insulin by radioimmunoassay (rat insulin RIA kit, Linco Research, St Charles, MO, USA) using 100 µl of plasma. The Homeostasis Model Assessment index (HOMA) was used as an index of insulin resistance and calculated with the following formula: [insulin (µU/ml) x glucose (mM)/22.5] [14].

Measurement of systolic blood pressure

Systolic arterial blood pressure was measured by tail-cuff plethysmography (Harvard Apparatus Ltd, Kent, UK) with the use of a cuff placed around the tail and registered on a MacLab/8 system. For each measurement, three individual readings were averaged [2,3].

Measurement of Allodynia

Tactile and cold allodynia were assessed with the rats placed on a wire mesh floor beneath an inverted plastic cage. The rats were allowed to adapt for about 15 min or until explorative behaviour ceased. Tactile allodynia was assessed by measuring the hindpaw withdrawal threshold to the application of a calibrated series of six von Frey filaments (bending forces of 2, 4, 6, 8, 10 and 15 g) applied perpendicularly to the mid-plantar surface as described previously [1,2,3]. Cold allodynia was assessed using the acetone drop method applied to the plantar surface of the hindpaws as previously described [1,2,3]. The frequency of paw withdrawal was expressed as a percentage (the number of paw withdrawals ÷ number of trials ×100).

Measurement of superoxide anion and NADPH oxidase activity in the aorta

Superoxide anion ($O_2^{\bullet-}$) production was measured in frozen isolated thoracic aorta rings using the lucigenin-enhanced chemiluminescence method as described previously [15,16]. Briefly, isolated aortas cut in 2–5 mm rings were pre-incubated at 37°C for 30 min in Krebs-HEPES buffer (saturated with 95% O_2 and 5% CO_2). Aortic rings were then transferred in duplicate to glass scintillation vials containing 200 µl of lucigenin (5 µM), which was previously dark adapted for 30 min. The chemiluminescence was recorded every minute for 10 min at room temperature using a liquid scintillation counter (Wallac 1409; Perkin Elmer Life Science, St Laurent, Quebec, Canada). Lucigenin counts were expressed as counts per minute per milligram of dry weight tissue (cpm/mg). The estimation of NADPH oxidase activity was achieved by adding to the aorta vials NADPH (10^{-4} M) before counting for another 6 min. Basal superoxide-induced luminescence was subtracted from the luminescence value induced by NADPH. Background counts were determined from vessel-free incubation media containing lucigenin and subtracted from the readings obtained with vessels.

Experiments designed to study the source of $O_2^{\bullet-}$ were carried out as indicated above in freshly isolated aorta with the addition of vehicle or one of the following inhibitors: N^{ω}-nitro-L-arginine methyl ester (L-NAME,100 µM, nitric oxide synthase inhibitor) [17], allopurinol (100 µM, xanthine oxidase inhibitor) [16], apocynin (10 µM, NADPH oxidase inhibitor) [18]. One hour

later, the B_1R agonist Sar[D-Phe^8]des-Arg^9-BK (20 μM) [19] was added to the solution for a further period of 15 min. In vivo experiments were also carried out in glucose-fed rats in which the B_1R agonist Sar[D-Phe^8]des-Arg^9-BK (1 mg/kg, i.p.) was administered 30 min after apocynin (50 mg/kg, i.p.). After a systemic exposure of 30 min to the B_1R agonist or its vehicle, rats were sacrificed under CO_2 inhalation, the aortas isolated and processed for $O_2^{\bullet-}$ measurement as indicated above.

The in situ level of $O_2^{\bullet-}$ in the aorta was also evaluated by the oxidative fluorescent dye dihydroethidine as described earlier [20]. Cells are permeable to dihydroethidine and, in the presence of $O_2^{\bullet-}$, it is oxidized to fluorescent ethidium bromide (EtBr) which is trapped by intercalation with DNA. EtBr is excited at 518 nm with an emission spectrum of 605 nm. Unfixed frozen aorta segments from the four experimental groups of rats (4 controls, 4 controls + SSR240612, 4 glucose-treated, 4 glucose-treated + SSR240612) were cut into 20-μm thick sections and placed on glass slides. Dihydroethidine (2 μM) was applied to tissue sections and coverslipped. The slides were then incubated in a light-protected humidified chamber at 37°C for 30 min. Images were obtained with a Leica TCS SP confocal microscope equipped with an argon laser (Leica microsystem Co., Germany). Tissues from the four groups were processed and imaged in parallel. Laser settings were identical for acquisition of images from all sections. Computer based analysis was performed with Image J software and calculated by the following equation: $I = \sum I/(A/N)$, where I is the fluorescence intensity, $\sum I$ is the summation of all nuclei intensity, A is the total area of the nuclei, and N is the number of nuclei used. Data are expressed as an average of total nuclei fluorescence quantified in triplicate of 4 rats.

Real-time quantitative polymerase chain reaction (qRT-PCR)

Once the blood was collected after sacrifice, approximately 10 mg of each isolated tissue (thoracic aorta and spinal cord, liver, gastrocnemius muscle) were put in RNAlater stabilisation reagent (QIAGEN, Valencia, CA, USA). Total RNAs were extracted from tissue according to the manufacturer's instructions. First-strand cDNA synthesized from 400 ng total RNA with random hexamer primers was used as template for each reaction with the QuantiTect Rev Transcription Kit (QIAGEN). qRT-PCR was performed in SYBR Green Master mix (QIAGEN) with 300 nM of each primer and signal detected using a Mx3000p device (Stratagene, La Jolla, CA, USA) as described [21]. For standardization and quantification, rat 18S was amplified simultaneously. The primer pairs were designed by Vector NTI software (Table 1).

PCR conditions were: 95°C for 15 min, followed by 46 cycles at 94°C for 15 s, 60°C for 30 s and 72°C for 30 s. The cycle threshold (Ct) value represents the cycle number at which a fluorescent signal rises statistically above background [22]. The relative quantification of gene expression was analyzed by the $2^{-\Delta\Delta Ct}$ method [23].

Density and distribution of kinin B_1 receptors by autoradiography

After sacrifice of rats, part of the thoracic spinal cord (T3–T7) was immediately frozen in 2-methylbutane cooled at −45 to −55°C with liquid nitrogen and kept at −80°C. Spinal cords were mounted in a gelatine block, serially cut into 20 μm thick coronal sections on a cryostat and stored at −80°C for 1 month. Thereafter sections were thawed at room temperature, pre-incubated for 10 min in 25 mM PIPES-NH_4OH buffer (pH 7.4) and then incubated at room temperature for 90 min in the same buffer containing peptidase inhibitors and 200 pM of [^{125}I]-HPP-desArg^{10}-Hoe 140 [2,3,24]. The non-specific binding was determined in the presence of 1 μM of the B_1 receptor antagonist: R715 (AcLys[D-ßNal^7,Ile^8]des-Arg^9-BK [6]. Kodak Scientific Imaging Films BIOMAX^{TM} MR® (Amersham Pharmacia Biotech Canada) were juxtaposed onto the slides in the presence of [^{125}I]-microscales and exposed at room temperature for 5–7 days. Autoradiograms were quantified by densitometry using an MCID^{TM} image analysis system. A standard curve from [^{125}I]-microscales was used to convert density levels into fentomoles per milligram of protein [25]. Specific binding was determined by subtracting values of non-specific binding from that of total binding. Total binding and non-specific binding were measured separately on 4 sections per rat with 6–8 rats per group.

Western blot analysis

Western blot analysis of protein expression was performed as described earlier [26]. After sodium dodecyl sulfate polyacrylamide gel electrophoresis (SDS-PAGE), the separated proteins were electrophoretically wet transferred to a nitrocellulose membrane (Bio-Rad) at 100 V for 1 h. After transfer, the membranes were washed twice in PBS-Tween 20 and incubated in PBS containing 5% skim milk at room temperature for 1 h. The blots were cut in pieces according to the molecular weight of the protein and then incubated with the specific antibodies for MnSOD (1/500, cat number: sc-18503), catalase (1/500, cat number: sc-34285), dynein (1/5000, cat number: sc-13524) and β-actin (1/10000, cat number A5441) in PBS-Tween 20 at 4°C overnight. Dynein and β-actin were used as standard proteins. After three washings in PBS-Tween 20 buffer, the membranes were incubated for 1 h at room temperature in PBS-Tween 20 containing 5% milk with secondary antibody that is bovine anti-goat IgG-HRP (1/5000, cat number: sc-2350) or anti-mouse IgG-HRP (1/5000, cat number sc-2005) (for β-actin and dynein). β-

Table 1. Primer pairs used in qRT-PCR analysis.

Gene	Sequences	Position	Gen Bank
B_1 receptor forward	5′GCA GCG CTT AAC CAT AGC GGA AAT 3′	367–391	NM_030851
B_1 receptor reverse	5′CCA GTT GAA ACG GTT CCC GAT GTT 3′	478–454	NM_030851
18S forward	5′TCA ACT TTC GAT GGT AGT CGC CGT 3′	363–386	X01117
18S reverse	5′TCC TTG GAT GTG GTA GCC GTT TCT 3′	470–447	X01117
MnSOD forward	5′ACG CGA CCT ACG TGA ACA ATC TGA 3′	175–198	Y00497
MnSOD reverse	5′TCC AGC AAC TCT CCT TTG GGT TCT 3′	367–344	Y00497

doi:10.1371/journal.pone.0012622.t001

actin antibody was purchased from Sigma-Aldrich Canada while other antibodies were from Santa Cruz Biotechnology, CA, USA. The blots were then washed three times with PBS-Tween 20 before the reaction with enhanced-chemiluminescence, Western blotting detection reagents (Amersham). A quantitative analysis of the protein was performed by densitometric scanning of the autoradiographs employing the enhanced laser densitometer, LKB Ultroscan XL, and quantified using the gel-scan XL evaluation software (version 2.1) from Pharmacia (Baie d'Urfé, Quebec, Canada).

Drugs

The selective non-peptide B_1R antagonist SSR240612 ((2R)-2-[((3R)-3-(1,3-benzodioxol-5-yl)-3-{[(6-methoxy-2-naphtyl)sulfonyl]amino}propanoyl)amino]-3-(4-{[(2R,6S)-2,6-dimethylpiperidinyl]methyl}phenyl)-N-isopropyl-N-methylpropanamide,fumarate) was obtained from Sanofi-Aventis R&D (Montpellier, France) [12]. Sar[D-Phe^8]des-Arg^9-BK and HPP-des-Arg^{10}-Hoe140 (3-(4hydroxyphenyl)propionyl-desArg^9-D-Arg^0[Hyp^3,Thi^5,D-Tic^7,Oic^8]Bradykinin) were synthesized at the Research Institute of Biotechnology, National Research Council of Canada (Montreal, Quebec, Canada). R-715 was kindly provided by Dr D. Regoli (Pharmacology, University of Ferrara, Italy). Iodination of HPP-des-Arg^{10}-Hoe140 was performed with the chloramine T method as described earlier [24]. SSR240612 was dissolved in dimethyl sulfoxide (DMSO, 0.5% v/v) and then ethanol (5% v/v) and Tween-80 (5% v/v) were added in this sequence. The solution was completed in distilled water. The drug was administered orally by gavage in a volume of 1 ml per 100 g of body weight. D-Glucose, apocynin, allopurinol, NADPH, lucigenin and L-NAME were purchased from Sigma-Aldrich Canada. Dihydroethidine was obtained from Molecular Probes (Invitrogen Corporation, Carisbad, CA, USA) and suspended in DMSO at a concentration of 10^{-3} M, and stored at -20°C until use. Subsequent dilutions were made in PBS. All other chemicals used were purchased from standard commercial suppliers and were of analytical grade.

Statistical analysis of data

Data are expressed as mean ± s.e.m of values obtained from (n) rats in each group. Statistical analysis of data was calculated with GraphPad Prism (version 4.00) software. Statistical differences were evaluated with Student's t-test on unpaired samples (B_1R binding sites). Multiple comparisons were analysed using one-way or two-way analysis of variance (ANOVA), followed by the Bonferroni post-test. Only probability values (P) less than 0.05 were considered to be statistically significant.

Results

Acute effect of SSR240612 on systolic blood pressure

Systolic blood pressure was significantly increased ($P<0.001$, $n = 6–12$) in the four groups of 12-week glucose-treated rats when compared to control rats and was dose-dependently reduced by the oral administration of SSR240612 (Baseline values of Glucose + vehicle: 151.2±5.7 mmHg; Glucose + SSR240612 (3 mg/kg): 152.2±2.0 mmHg; Glucose + SSR240612 (10 mg/kg): 160.4± 3.2 mmHg; Glucose + SSR240612 (30 mg/kg): 156.5±4.7 mmHg; Control + SSR240612 (10 mg/kg): 125.3±3.3 mmHg; Control + SSR240612 (30 mg/kg): 129.7±1.9 mmHg) (Figure 1A). When the area under the curve was measured between 0 h to 48 h post-administration, the dose of 3 mg/kg did not reach statistical significance. However, doses of 10 and 30 mg/kg SSR240612 decreased significantly high blood pressure when compared with vehicle ($P<0.05$). In contrast, doses of 10 and 30 mg/kg

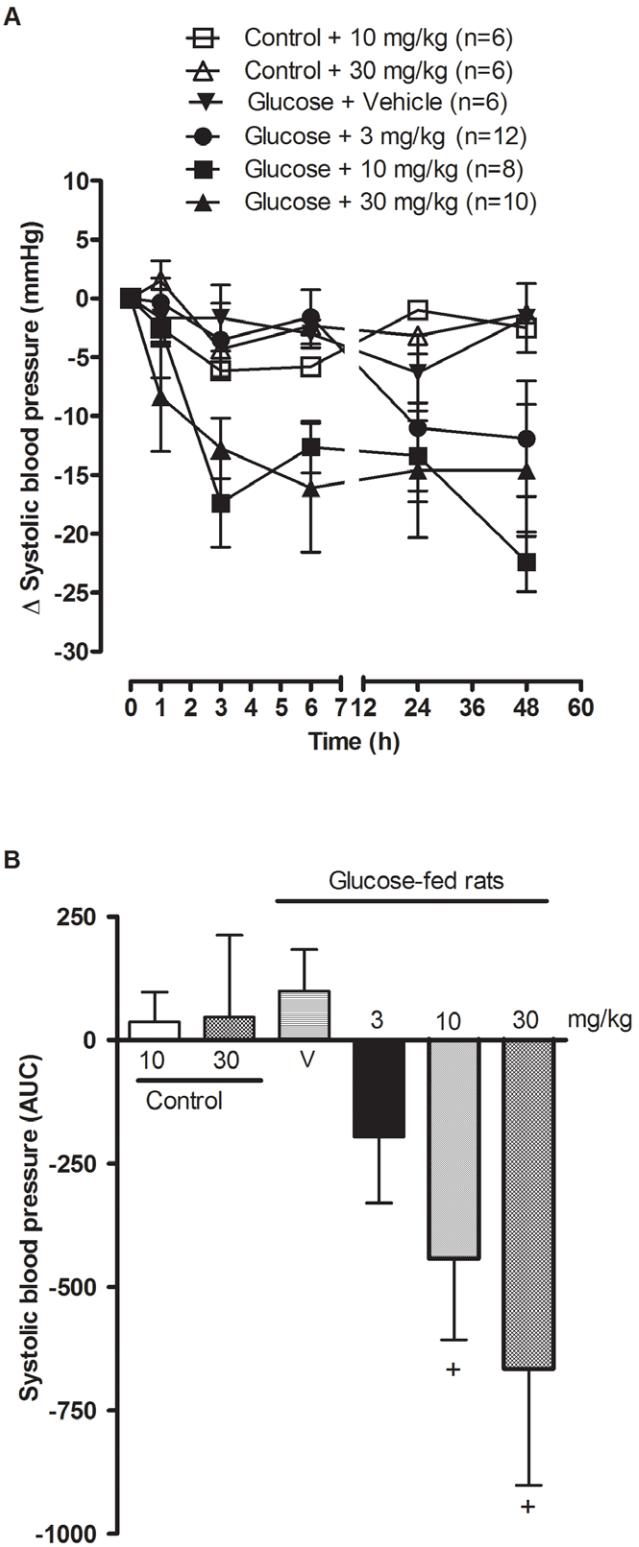

Figure 1. Acute effect of orally administered SSR240612 on systolic blood pressure in 12-week glucose-fed rats. Doses of 10 mg/kg and 30 mg/kg of SSR240612 were given to control rats and doses of 3, 10, 30 mg/kg of SSR240612 or vehicle were given to glucose-fed rats. Data are mean ± s.e.m of values obtained from (n) rats and represent changes of systolic blood pressure in mmHg (A) or Area Under the Curve (B). Statistical comparison with vehicle (V) in glucose-fed rats (+) is indicated by + $P< 0.05$.
doi:10.1371/journal.pone.0012622.g001

SSR240612 administered to control rats had no significant effect on systolic blood pressure (Figure 1B). Therefore, the dose of 10 mg/kg SSR240612 was selected for chronic treatment in the remainder of the study.

Chronic effect of SSR240612 on systolic blood pressure

As shown in figure 2, systolic blood pressure was significantly higher ($P<0.001$) in glucose-fed rats when compared to age-matched control rats. A one-week treatment with SSR240612 (10 mg/kg) reduced significantly high blood pressure in glucose-fed rats at 6 h on day 0 and during the remaining period of treatment when compared to age-matched glucose-fed rats receiving the vehicle. The reduction of blood pressure was incomplete during the premier 2 days of treatment but became sustained and reached control values from day 3 to day 7. In contrast, the same treatment with SSR240612 for a period of one week had no significant effect on systolic blood pressure in control rats when compared to untreated control rats.

Chronic effect of SSR240612 on allodynia

As shown in figure 3A, glucose-fed rats displayed significant and sustained tactile allodynia ($P<0.001$) when compared to age-matched control rats from day 0 to day 7. Chronic treatment with 10 mg/kg SSR240612 caused a significant reduction of tactile allodynia in glucose-fed rats at 3 and 6 h post-gavage on day 0 when compared to glucose-fed rats treated with vehicle. The inhibition was entirely reversible at 24 h but not on the subsequent days until the completion of the treatment on day 7. The higher paw withdrawal threshold occurring between day 3 to day 7 in glucose-fed rats treated with SSR240612 was not significantly different from control values. Finally, daily administration of 10 mg/kg SSR240612 for 7 days had no significant effect on paw-withdrawal threshold to tactile stimulation in control rats when compared to untreated control rats.

As shown in figure 3B, glucose-fed rats also displayed significant cold allodynia ($P<0.001$) when compared to age-matched control rats from day 0 to day 7. Significant reduction of cold allodynia was seen at 3 and 6 h after treatment with 10 mg/kg SSR240612 on day 0 when compared to glucose-fed rats treated with vehicle. This inhibition was no longer significant at 24 h. On the following days, daily treatment with SSR240612 led to a striking and irreversible inhibition of cold allodynia. From day 2 to day 7, response frequency to cold stimulation was not significantly different between control and glucose-fed rats treated with SSR240612. In contrast, the same treatment with SSR240612 for one week had no significant effect on paw-withdrawal threshold to cold stimulation in control rats when compared to untreated control rats.

Chronic effect of SSR240612 on various parameters

As shown in table 2, body weight was not significantly different between the four groups. Plasma levels of glucose and insulin were significantly increased in rats fed with 10% D-Glucose when compared with age-matched control rats. Plasma glucose levels in glucose-fed rats treated for 1 week with 10 mg/kg SSR240612 were not significantly different from control values. High plasma insulin levels were significantly reduced in glucose-fed rats treated with SSR240612 when compared with glucose-fed rats treated with vehicle. Insulin resistance as assessed by the HOMA index was increased by 5.6-fold in glucose-fed rats when compared with age-matched control rats. This value was significantly reduced though not completely normalised by one-week treatment with SSR240612. The same regimen with SSR240612 failed to affect plasma levels of glucose and insulin and the HOMA index in control rats. Water intake was increased by 2-fold in glucose-fed

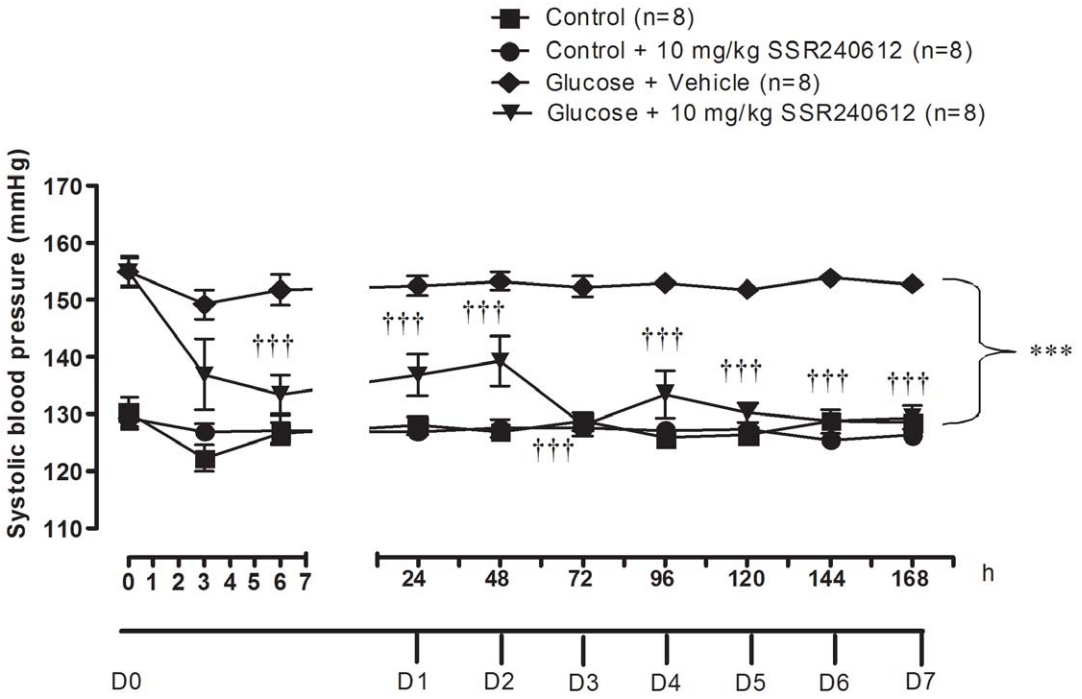

Figure 2. Effect of orally administered SSR240612 (10 mg/kg/day for 7 days) on systolic blood pressure in glucose-fed rats. From day (D) 1 to 7, measurements were taken prior to the morning treatment with SSR240612. Data are mean ± s.e.m of values obtained from (n) rats. Statistical comparison with controls (*) or glucose-fed rats + vehicle (†) is indicated by ***†††$P< 0.001$.
doi:10.1371/journal.pone.0012622.g002

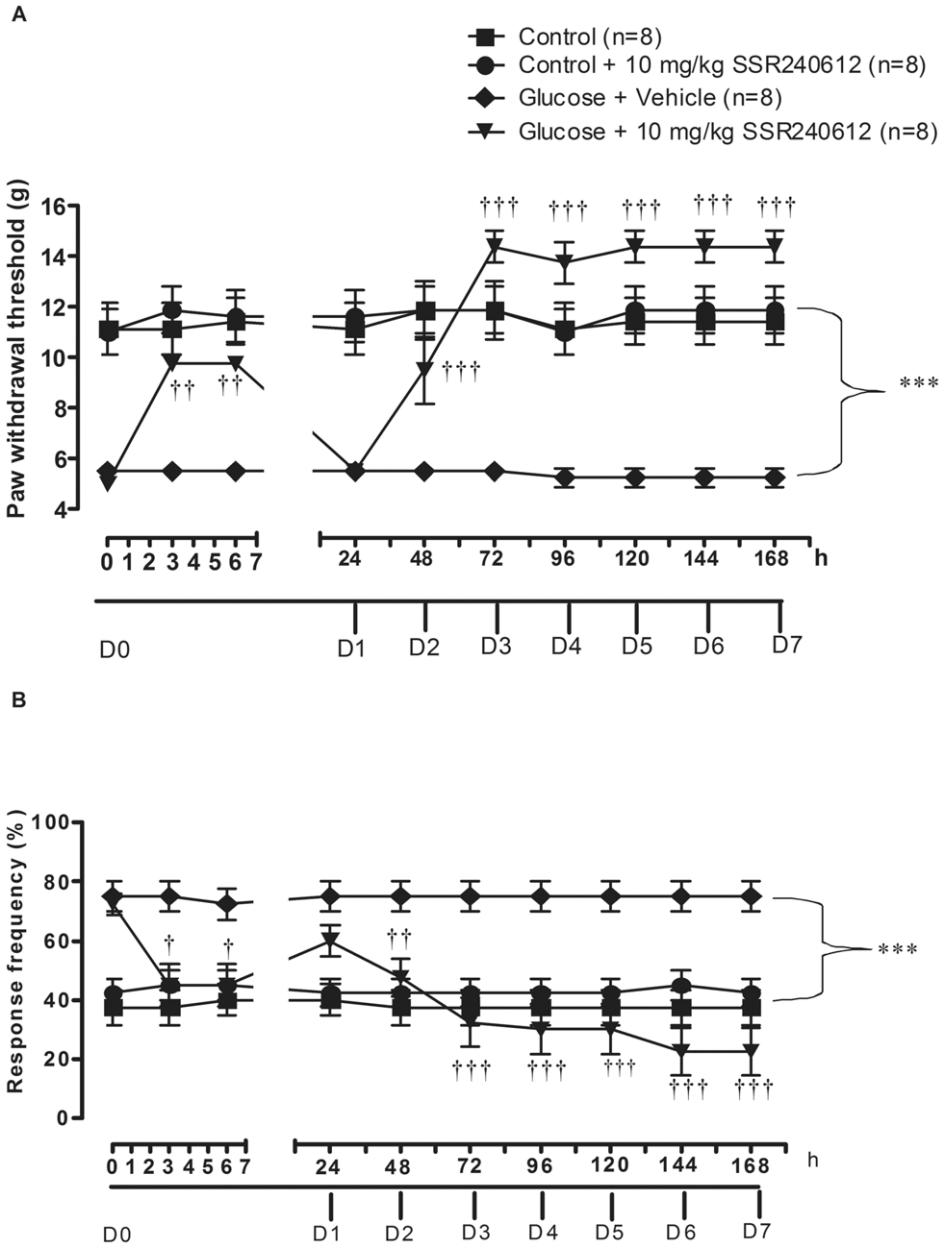

Figure 3. Effect of orally administered SSR240612 (10 mg/kg/day for 7 days) on (A) tactile allodynia and (B) cold allodynia in glucose-fed rats. From day (D) 1 to 7, measurements were taken prior to the morning treatment with SSR240612. Data are mean ± s.e.m of values obtained from (n) rats. Statistical comparison with controls (*) or glucose-fed rats + vehicle (†) is indicated by †P< 0.05, ††P< 0.01, ***†††P< 0.001.
doi:10.1371/journal.pone.0012622.g003

Table 2. Effects of SSR240612 (10 mg/kg/day ×7 days) in rats treated with glucose.

Parameters	Control n = 6	Control + SSR240612 n = 6	Glucose-fed + Vehicle n = 8	Glucose-fed + SSR240612 n = 8
Body weight (g)	392.0±12.3	397.2±5.9	408.4±7.3	387.6±12.9
Plasma glucose (mmol/L)	5.8±0.2	6.3±0.2	7.8±0.8 *	6.6±0.4
Plasma insulin (ng/ml)	1.0±0.3	0.8±0.2	7.0±1.4 ***	2.1±0.3 ** †††
HOMA index	5.2±1.3	4.9±1.1	29.2±2.8 ***	10.4±1.8 * †††
Drinking (ml)	58.2±2.2	59.7±1.2	119.1±5.0 **	112.6±8.5 **
Food intake (g)	30.9±0.2	30.6±0.2	20.7±1.1 **	22.5±0.8 **

Values represent the mean ± s.e.m of (n) rats. Statistical comparison to control rats (*) or to glucose + vehicle (†) is indicated by * P<0.05;** P<0.01; *** ††† P<0.001.
doi:10.1371/journal.pone.0012622.t002

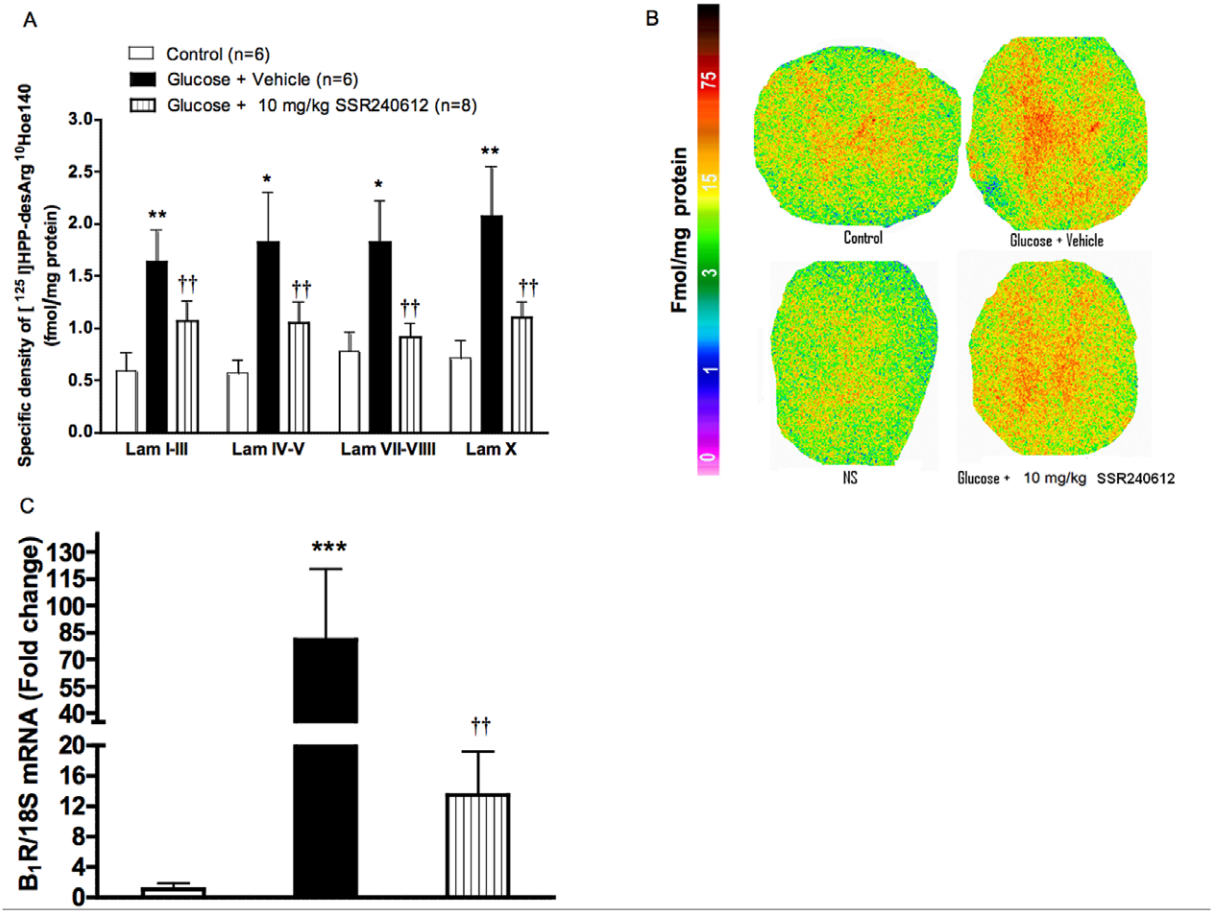

Figure 4. Effect of orally administered SSR240612 (10 mg/kg/day for 7 days) on B_1R expression in the thoracic spinal cord. A: Quantification of specific density of [^{125}I]-HPP-desArg^{10}-Hoe 140 to B_1R in various spinal cord laminae (Lam). B: Autoradiograms of thoracic spinal cord for B_1R. The non-specific binding (NS) was obtained by the co-addition of 1 µM R-715 (B_1R antagonist) with [^{125}I]-HPP-desArg^{10}-Hoe 140. C: Bars represent fold change in gene expression for B_1R. Data are mean ± s.e.m of values obtained from (n) rats. Statistical comparison with controls (*) or glucose-fed rats + vehicle (†) is indicated by * $P< 0.05$, **††$P< 0.01$, ***$P< 0.001$.
doi:10.1371/journal.pone.0012622.g004

rats and this was compensated by a 33% reduction of food intake. SSR240612 treatment for 7 days had no effect on drinking or eating behaviour in both glucose-fed rats and controls rats (Table 2).

Chronic effect of SSR240612 on B_1R binding sites and B_1R mRNA in spinal cord

Quantitative autoradiography showed a significant increase of specific density of kinin B1R binding sites through laminae I to X of the thoracic spinal cord in glucose-fed rats when compared to age-matched control spinal cord (Figure 4A and 4B). This overexpression of B1R binding sites in glucose-fed rats was significantly reduced in all laminae by the one-week treatment with 10 mg/kg SSR240612. As shown in figure 4C, B1R mRNA was underexpressed in the spinal cord of control rats. In glucose-fed rats, however, B1R mRNA was increased by 80-fold. Again, the overexpression of B1R mRNA in the spinal cord of glucose-fed rats was significantly and markedly decreased by SSR240612.

Chronic effect of SSR240612 on B_1R mRNA levels in peripheral organs

Similarly to the spinal cord, levels of B1R mRNA were relatively low in aorta, liver and gastrocnemius muscle of control

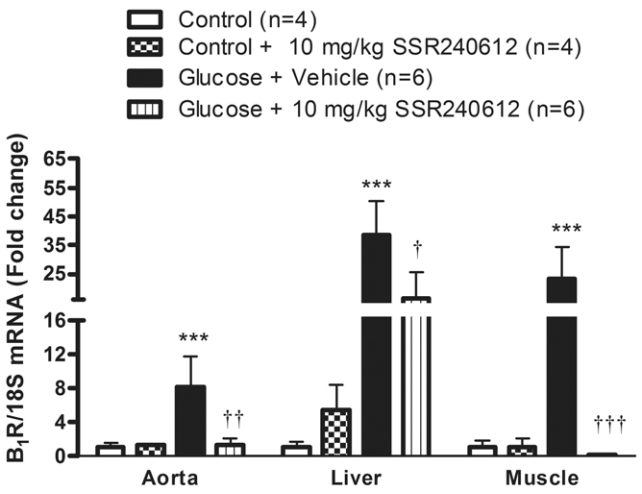

Figure 5. B_1R mRNA levels in aorta, liver and skeletal muscle after orally administered SSR240612 (10 mg/kg/day for 7 days). Data are mean ± s.e.m of values obtained from (n) rats. Statistical comparison with controls (*) or glucose-fed rats + vehicle (†) is indicated by † $P< 0.05$, ††$P< 0.01$, ***†††$P< 0.001$.
doi:10.1371/journal.pone.0012622.g005

rats (Figure 5). However in glucose-fed rats, B1R mRNA levels were markedly and significantly upregulated in the same tissues. The one-week treatment with 10 mg/kg SSR240612 reversed completely B1R mRNA overexpression in aorta and skeletal muscle and reduced significantly B1R mRNA level in the liver of glucose-fed rats. The antagonist was without effect on the basal expression of B1R mRNA in control rats.

Chronic effect of SSR240612 on oxidative stress

Effects of 8-week treatment with glucose on basal and NADPH-stimulated $O_2^{\bullet-}$ production measured in the aorta using lucigenin-enhanced chemiluminescence are shown in figure 6. Glucose feeding resulted in a 1.9-fold increase of basal $O_2^{\bullet-}$ production in the aorta when compared to control aorta (Figure 6A). The one-week treatment with SSR240612 normalised the higher production of $O_2^{\bullet-}$ in glucose-fed rats to control levels. SSR240612 failed, however, to alter basal $O_2^{\bullet-}$ production in the aorta of control rats (Figure 6A). Moreover, NADPH oxidase activity was significantly increased by 2-fold in the aorta of glucose-fed rats. Again, the increase of NADPH oxidase activity in glucose-fed rats was significantly reduced by the one-week treatment with SSR240612. The latter treatment with the B_1R antagonist failed to alter $O_2^{\bullet-}$ production induced by NADPH in the aorta of control rats (Figure 6B).

The production of $O2^{\bullet-}$ evaluated with the oxidative fluorescent dye dihydroethidine was also markedly increased in vascular smooth muscle cells of the aorta in glucose-fed rats (Figures 7C and 8). Daily treatment with 10 mg/kg SSR240612 for a week abolished the fluorescent labelling seen in the aorta of glucose-fed rats to control levels (Figures 7D and 8). However, the weak labelling displayed in the aorta of control rats was not affected by the B1R antagonist (Figures 7A-B and 8).

Pro-oxidative effect of B_1R

To further substantiate the contribution of B1R in the production of $O2^{\bullet-}$, aortas from glucose-fed rats were incubated in the presence of the B1R agonist Sar[D-Phe8]des-Arg9-BK (20 μM). Results presented in figure 9 show that the B1R agonist

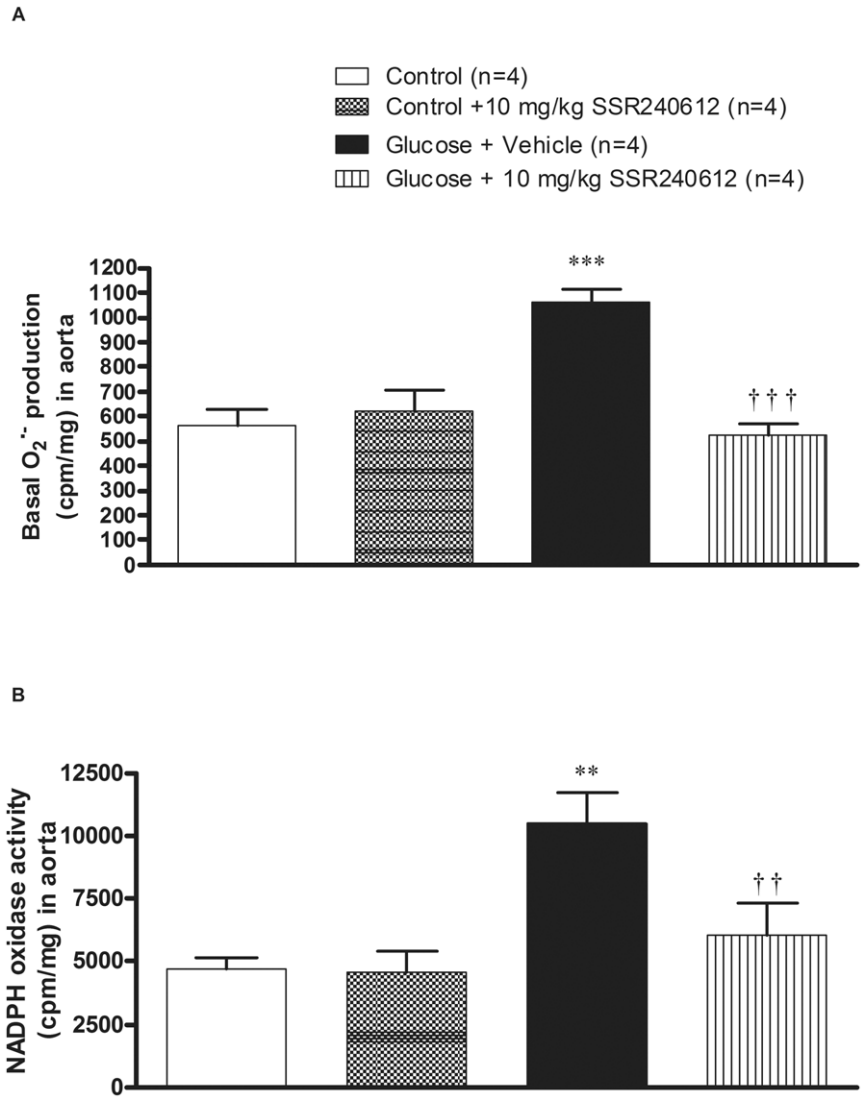

Figure 6. Effect of orally administered SSR240612 (10 mg/kg/day for 7 days) on oxidative stress. (A) Basal superoxide anion production, (B) NADPH oxidase activity in the aorta of glucose-fed rats. Data are mean ± s.e.m of values obtained from (n) rats. Statistical comparison with controls (*) or glucose-fed rats + vehicle (†) is indicated by **††P< 0.01, ***†††P< 0.001.
doi:10.1371/journal.pone.0012622.g006

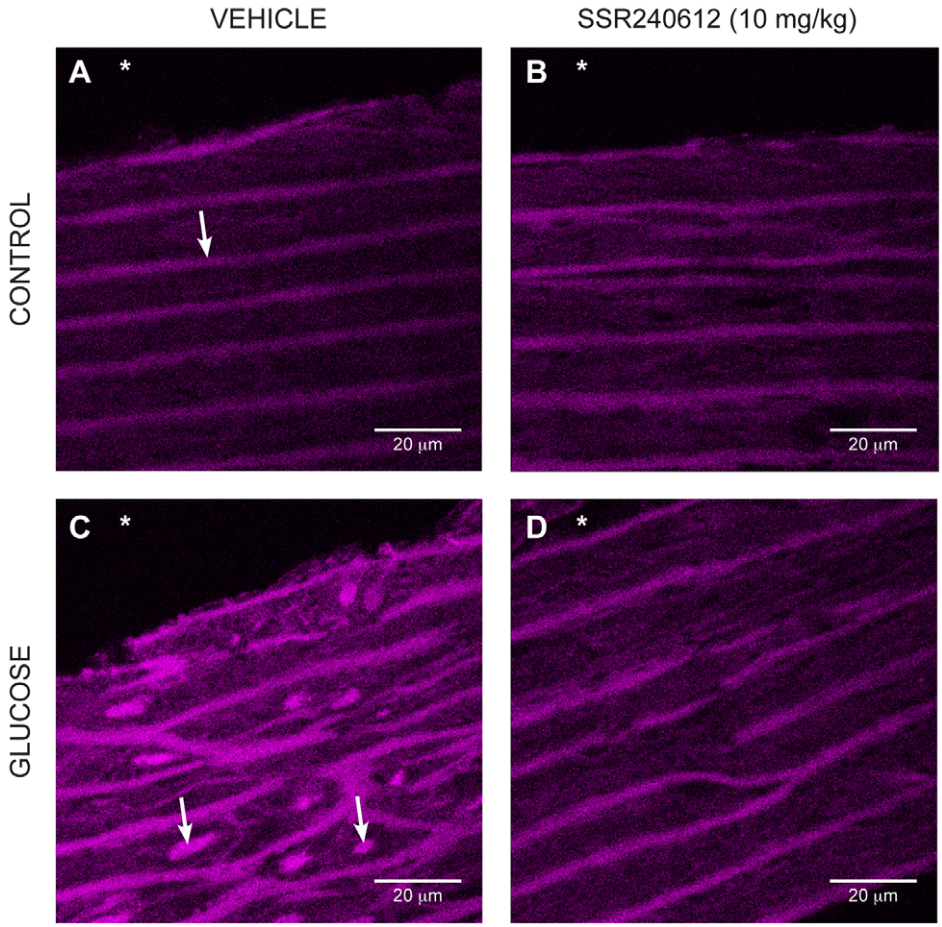

Figure 7. Superoxide anion production on histological sections of the aorta marked with dihydroethidine. Control (A, B) and glucose-treated rats (C, D) after 7-day treatment with Vehicle (A, C) or 10 mg/kg/day SSR240612 (B, D). Asterisk (*) indicates the lumen side of the section. The arrow (in A) represents the elastic lamina of the smooth muscle cells while the two arrows (in C) show the increase of fluorescent ethidium bromide in the nucleus of smooth muscle cells in the aorta of glucose-treated rat. The fluorescent marker is reduced after treatment with SSR240612 (in D). Scale bar is 20 μm in each panel. Images are representative of 4 aortas in each group.
doi:10.1371/journal.pone.0012622.g007

enhanced by 4-fold the production of $O2^{\bullet-}$. Whereas the pro-oxidative response to Sar[D-Phe8]des-Arg9-BK was not significantly affected by allopurinol (xanthine oxidase inhibitor) and L-NAME (a non-selective inhibitor of all NOS isoforms), it was completely blocked by apocynin (NADPH oxidase inhibitor). Baseline values of $O2^{\bullet-}$ production in glucose-treated aortas were either slightly reduced (L-NAME) or normalized (apocynin and allopurinol) by these inhibitors.

The intraperitoneal administration of Sar[D-Phe8]des-Arg9-BK (1 mg/kg) in 8-week glucose-fed rats also enhanced by 4-fold the production of $O2^{\bullet-}$ in aorta (Figure 10). Similarly to the *in vitro* protocol, systemic treatment with apocynin (50 mg/kg) abolished the effect of the B1R agonist on the production of $O2^{\bullet-}$. It is worth mentioning that apocynin normalized the increasing effect of glucose on baseline $O2^{\bullet-}$ production. These findings suggest that B1R activation can increase the production of superoxide anion primarily through NADPH oxidase.

Chronic effect of SSR240612 on superoxide dismutase and catalase expression

The impact of SSR240612 was evaluated on the vascular antioxidant defence. Firstly, the mRNA and protein expressions of MnSOD were markedly increased in the aorta of glucose-fed rats when compared to age-matched control rats (Figure 11A and 11B). The up-regulation of this antioxidant enzyme was reversed (mRNA) or significantly reduced (protein) by the one-week treatment with 10 mg/kg SSR240612. Secondly, the protein expression of catalase was significantly increased in the aorta of 8-week glucose-fed rats and the one-week treatment with SSR240612 reduced it significantly (Figure 12). In contrast, the prolonged treatment with the B_1R antagonist had no significant effect on MnSOD or catalase expression in the aorta of control rats (Figures 11–12).

Discussion

This study provides the first demonstration that the activation of B_1R increased the oxidative stress through the activation of NADPH oxidase in the vasculature and that the sustained inhibition of B_1R for one-week with SSR240612 reversed the oxidative stress and the subsequent B_1R upregulation in a model of insulin resistance. Indeed, activation of B_1R with a selective agonist either *in vitro* or *in vivo* enhanced the production of aortic superoxide anion which was abolished by apocynin, a selective inhibitor of NADPH oxidase. The inhibition of B_1R had positive outcome on diabetic complications in the model of glucose-fed rat.

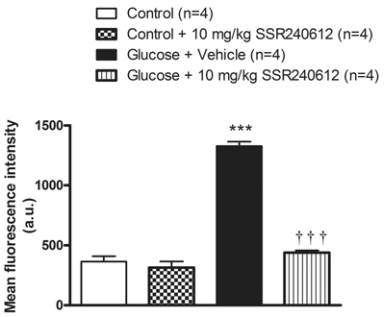

Figure 8. Fluorescence intensities of superoxide (dihydroethidium) staining in aortic sections from control and 8-week glucose-treated rats shown in Figure 7. Data are expressed as fluorescence intensity in arbitrary unit (a.u.) and represent the mean ± s.e.m of 4 rats in each group. Statistical comparison with controls (*) or glucose-fed rats + vehicle (†) is indicated by ***†††P< 0.001.
doi:10.1371/journal.pone.0012622.g008

SSR240612 treatment had no effect on drinking and food intake in both control and glucose-fed rats, excluding an indirect effect of the drug on glucose intake.

Our findings on B_1R-induced allodynia are in keeping with the role of B_1R in hyperalgesia in inflammatory, diabetic and painful processes [27,28,29] and with the therapeutic effect of SSR240612 in neuropathic and inflammatory pain [12,30].

Relationship between oxidative stress, B_1R and glucose-induced hypertension and allodynia

It is known that diets containing high refined carbohydrates such as fructose, sucrose and glucose elevate blood pressure in rats [10,31,32,33]. Simple carbohydrate feeding to rat and high glucose infusion for 2 days elevate reactive oxygen species (ROS) [9,34,35]. Increased production of $O_2^{\bullet-}$ is correlated with high blood pressure in glucose-fed rats [8,9]. Alpha-lipoic acid attenuates aortic and heart mitochondrial $O_2^{\bullet-}$ production in glucose-fed rats [7,10] and reverses hypertension in fructose and glucose-fed rats [2,10,36]. The antioxidant N-acetyl-L-cysteine

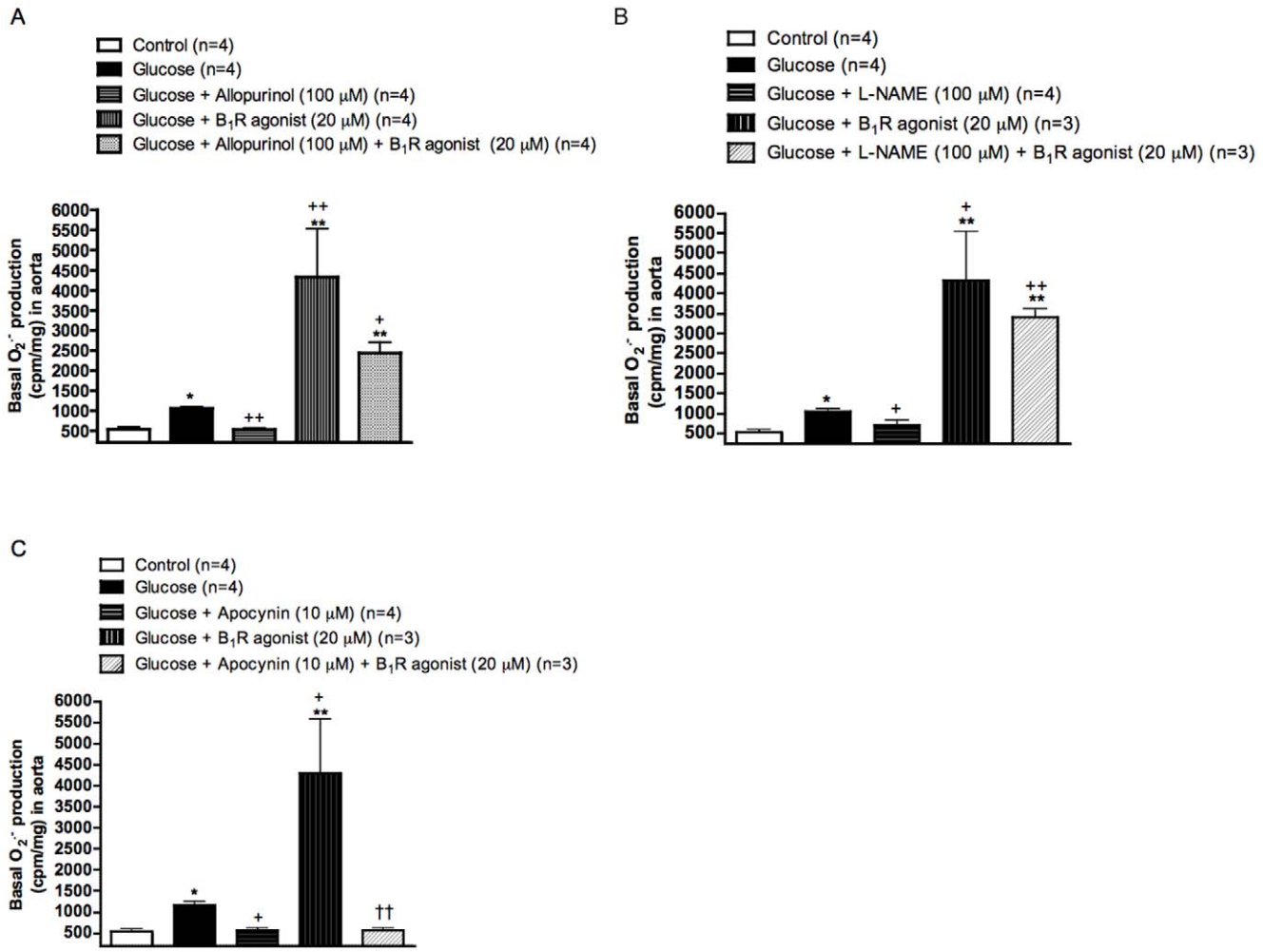

Figure 9. Effects of *in vitro* B_1R activation on superoxide anion production in the aorta of glucose-fed rats pre-treated or not with oxidative enzyme inhibitors. Basal and stimulated production of superoxide anion in the presence of the B_1R agonist Sar[D-Phe^8]des-Arg^9-BK (20 μM) were measured in the presence of (A) Allopurinol (xanthine oxidase inhibitor), (B) L-NAME (inhibitor of all NOS isoforms) and (C) Apocynin (NADPH oxidase inhibitor) at the indicated concentrations (see methods). Data are mean ± s.e.m of values obtained from (n) rats. Statistical comparison with control (*), glucose (+) or Sar[D-Phe^8]des-Arg^9-BK (†) is indicated by * $^+$ P< 0.05, ** $^{++}$ ††P< 0.01.
doi:10.1371/journal.pone.0012622.g009

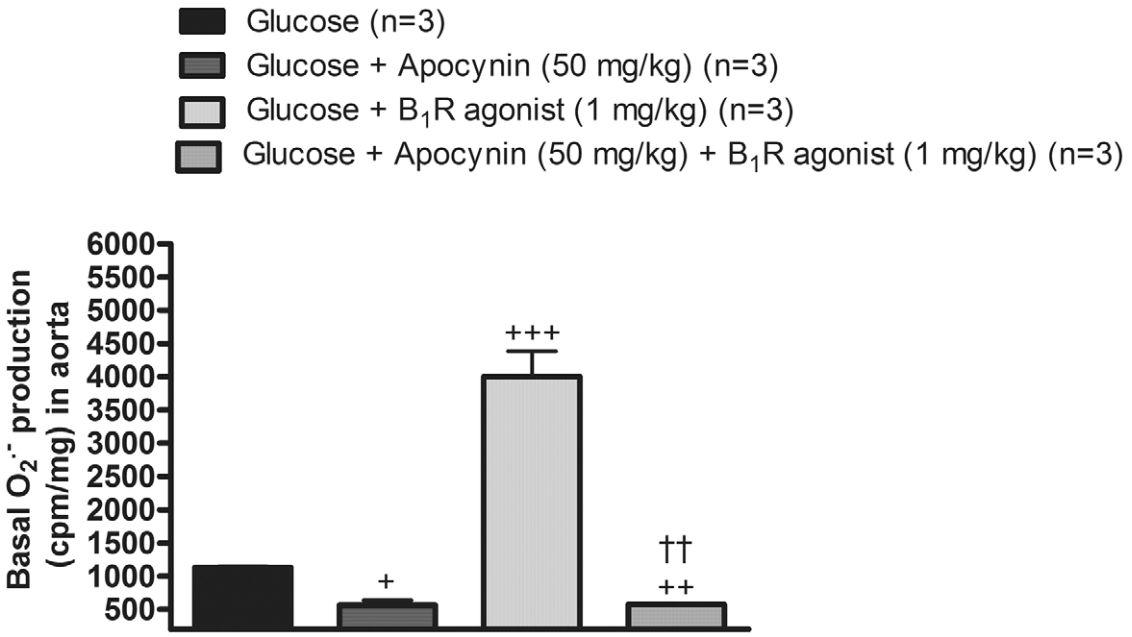

Figure 10. Effects of *in vivo* B_1R activation on superoxide anion production in the aorta of glucose-fed rats pre-treated or not with the NADPH oxidase inhibitor. Basal and stimulated production of superoxide anion with the B_1R agonist Sar[D-Phe^8]des-Arg^9-BK (1 mg/kg, i.p.). Apocynin (50 mg/kg, i.p.) was administered 30 min prior to the B_1R agonist (see methods). Data are mean ± s.e.m of values obtained from (n) rats. Statistical comparison with glucose (+) or Sar[D-Phe^8]des-Arg^9-BK (†) is indicated by $^{+}$ $P< 0.05$, $^{++}$ $^{††}P< 0.01$, $^{+++}P< 0.001$.
doi:10.1371/journal.pone.0012622.g010

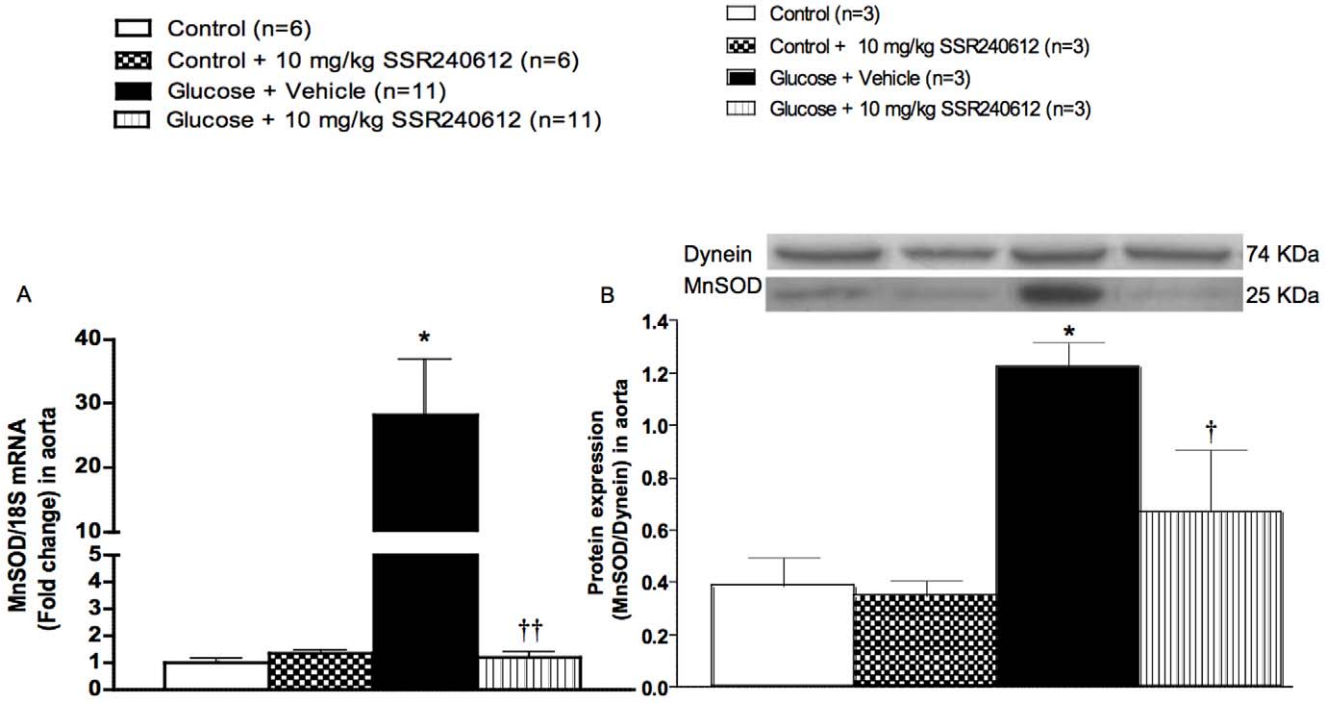

Figure 11. Effect of orally administered SSR240612 (10 mg/kg/day for 7 days) on vascular expression of superoxide dismutase. The expression of MnSOD was measured at (A) mRNA level by qRT-PCR, and (B) at protein level by Western blot in the aorta of glucose-fed rats. Data are mean ± s.e.m of values obtained from (n) rats. Statistical comparison with controls (*) or glucose-fed rats + vehicle (†) is indicated by $^{*†}P< 0.05$, $^{††}P< 0.01$.
doi:10.1371/journal.pone.0012622.g011

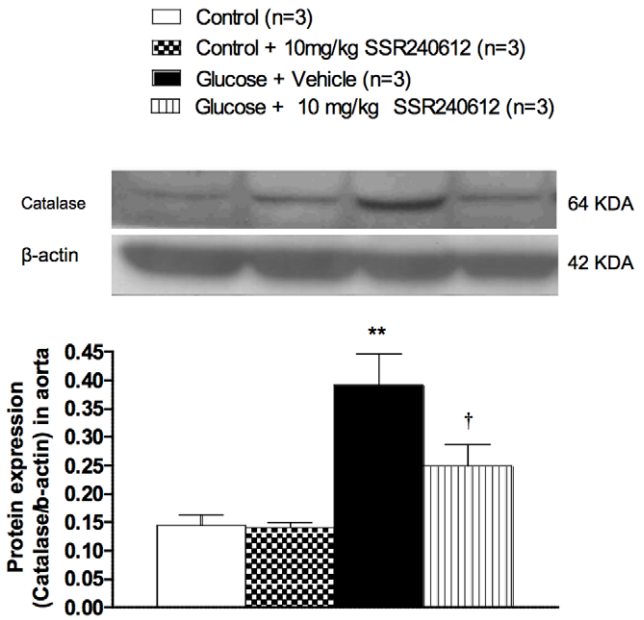

Figure 12. Effect of orally administered SSR240612 (10 mg/kg/day for 7 days) on vascular expression of catalase. The expression of catalase was measured at protein level by Western blot in the aorta of glucose-fed rats. Data are mean ± s.e.m of values obtained from (n) rats. Statistical comparison with controls (*) or glucose-fed rats + vehicle (†) is indicated by $^{\dagger}P< 0.05$, $^{**}P< 0.01$.
doi:10.1371/journal.pone.0012622.g012

also prevents high blood pressure in fructose and glucose feeding rats [3,37].

It is also well established that increased oxidative stress causes diabetic neuropathy, especially through the polyol pathway (high activity of the aldose reductase). Hyperglycemia induces nerve loss and reduces nerve velocity through oxidative stress. These problems are alleviated by alpha-lipoic acid [38]. In our model of high glucose feeding, alpha-lipoic acid and N-acetyl-L-cysteine were able to reduce simultaneously vascular oxidative stress, B_1R upregulation, hypertension and allodynia [2,3,7]. This is consistent with the increased B_1R mRNA and protein expression following a 12 h exposure of mesenteric vascular endothelial cells with 25 mM glucose [39]. The corollary of these findings is that the oxidative stress is likely the primary mechanism involved in the induction of B_1R in the model of insulin resistance induced by high glucose intake. The oxidative stress can activate the nuclear factor kappa B (NF-κB) pathway [40,41] which is directly involved in the upregulation of B_1R [4]. B_1R may therefore represent a molecular marker of the oxidative stress.

Source of superoxide anion and pro-oxidative effect of B_1R in glucose-fed rats

The NADPH oxidase is a predominant source of ROS production ($O_2^{\bullet-}$) in cardiovascular tissues in response to high glucose, growth factors and vasoactive peptides [42,43,44]. NADPH oxidase activity and $O_2^{\bullet-}$ levels were increased in cultured vascular smooth muscle cells exposed to high glucose concentration [45], in animal and clinical models of hypertension and diabetes [42,44,46]. In our study, the complete inhibition of increased glucose-induced superoxide anion by apocynin confirmed the predominant contribution of NADPH oxidase. However, the complete inhibition $O_2^{\bullet-}$ levels with allopurinol and its partial inhibition with L-NAME suggest multiple sources of ROS in this model, including xanthine oxidase and uncoupling eNOS. Xanthine oxidase was also proposed as a source of ROS in the vasculature in models of hypertension [42]. Furthermore, the increased NADPH activity observed in the present study is in agreement with data reported in the aorta of db/db mice, a type 2 model of diabetes [46].

A key finding of the present study was the demonstration that a one-week treatment with SSR240612 reversed the vascular oxidative stress and normalized B_1R up-regulation in glucose-fed rats. This contrasts with the acute treatment with SSR240612 which did not affect $O_2^{\bullet-}$ production in aorta [1]. The inhibition of NADPH oxidase activity may represent a molecular mechanism by which SSR240612 reduces the oxidative stress. This statement is supported by the increased production of $O_2^{\bullet-}$ by the B_1R agonist in isolated aorta of glucose-fed rats, whose effect was sensitive to the NADPH oxidase inhibitor apocynin. This observation was confirmed in aorta isolated from glucose-fed rats treated *in vivo* with apocynin prior to the B_1R agonist. Xanthine oxidase and uncoupling eNOS are unlikely involved in $O_2^{\bullet-}$ production by the B_1R agonist since their respective inhibitors (allopurinol and L-NAME) did not affect significantly the pro-oxidative effect of the B_1R agonist despite they reduced glucose-induced oxidative stress. Thus the inhibition of the oxidative stress by SSR240612 is likely due to the inhibition of the NADPH dependent pro-oxidative effect of B_1R activation. The inhibition and down-regulation of B_1R-induced oxidative stress following chronically administered SSR240612 may explain the persistent normalization of high blood pressure, allodynia and insulin resistance in glucose-fed rats.

Antioxidant defence and SSR240612

It is generally believed that the exposure of cells to oxidative stress is associated with increased antioxidant enzyme activity [47]. Exposure of human endothelial cells to 20 mM glucose for 1–2 weeks increased mRNA expression of CuZnSOD and MnSOD [48]. Likewise, porcine aortic vascular smooth muscle cells cultured in 25 mM glucose for 10 days increased MnSOD mRNA expression [49]. SOD activity was similarly increased in the plasma of 3-week glucose-fed rats [10]. Moreover, SOD and catalase activity were significantly increased during the early stage of diabetes in streptozotocin-treated rats [50]. Thus, the increased expression of MnSOD and catalase in the aorta of 8-week glucose-fed rats is congruent with previous studies and may reflect a compensatory mechanism to the enhanced oxidative stress in glucose-fed rats. It is therefore logical that the reduction of the oxidative stress by chronic treatment with B_1R antagonist resulted in a normalization of the MnSOD and catalase expression. This further links B_1R to the generation of the oxidative stress and suggests that the inhibitory effect of SSR240612 on the antioxidant defence is indirect and likely due to the inhibition of the production of ROS.

Link between B_1R and angiotensin II (ANG II)

Endogenous ANG II was found to enhance B_1R expression via AT_1 receptor in endothelium of small cardiac arteries and cardiomyocytes in two-kidney-one-clip hypertensive rats [51]. Also the experimental model of hypertension induced by chronic infusion of ANG II induced B_1R expression in rat aorta [52] and spinal cord [53] as previously shown in cultured vascular smooth muscle [54] through a mechanism associated with the oxidative stress and NF-kB. ANG II can activate NF-κB through increases of vascular superoxide production following membrane NADPH oxidase activation [55,56]. NF-κB is the transcription factor that allows the increased expression of B_1R [57]. Likewise the model of

insulin resistance induced by glucose feeding, the anti-hypertensive effect of SSR240612 was recently demonstrated in ANG II-hypertensive rats and spontaneously hypertensive rats [58].

Putative role of B_2R and its relationship with B_1R expression

Acute treatment with the B_2R antagonist Icatibant (1 mg/kg) reversed allodynia but not hypertension in rats treated with D-glucose for 12 weeks [59]. Further studies are, however, necessary to determine the influence of B_2R on the oxidative stress-induced pathological changes in this model. In addition to its pro-nociceptive and pro-inflammatory effects, increasing evidence shows that the B_2R is nephro- and cardioprotective [60,61,62,63,64,65], partly due to nitric oxide (NO) release, and could contribute to the benefit of angiotensin 1-converting enzyme (ACE) inhibitors in models of diabetes and cardiovascular diseases [5,60,66,67].

Whereas the B_1R is associated with leptin resistance and obesity [13], its beneficial or detrimental role in cardiac ischemia remains conflicting [65,68,69,70] and recently, B_1R was found implicated in renal fibrosis [71]. The lack of both kinin B_1R and B_2R enhances diabetic complications, including nephropathy and neuropathy in Akita diabetic mice [64]. In addition, genetically diabetic mice that lack the B_2R develop a more severe kidney pathology by age 6 months and develop senescence-associated phenotypes by age 12 months [72,73]. However, the expression of B_1R is markedly enhanced in B_2R knockout mice [72,74]. Renal expression of B_2R is also significantly enhanced in B_1R knockout mice [75], suggesting that the absence of one kinin receptor is compensated by the over-expression of the remaining kinin receptor. Thus, investigation on the respective role of B_1R and B_2R in diabetes using genetically modified mice must be cautiously interpreted since it does not simply reflect the absence of a given receptor and may explain apparent contradiction with pharmacological studies. Furthermore, other important genes are affected by genetic deletion of either kinin receptor. For instance, genetic disruption of B_1R or B_2R and both receptors decreased ACE and ANG II AT_1R function and expression in mice abdominal aorta, indicating that kinin receptors regulate AT_1 receptors and ACE [76,77]. Moreover, B_2R knockout mice have increased ANG II AT_2R mRNA and protein expression that contributes to elevation of NO as compensatory protective mechanism in thrombosis [78]. Finally, our study addressed the role of B_1R in insulin resistance which corresponds to the early phase of diabetes. The therapy with B_1R antagonists in a more advanced phase of diabetes as in Akita diabetic mice remains to be clarified.

Conclusion

The present study provides the first evidence that the B_1R can perpetuate the oxidative stress by increasing the production of superoxide anion following the activation of NADPH oxidase in a model of insulin resistance. Prolonged inhibition of B_1R with SSR240612 reversed hypertension, pain polyneuropathy and metabolic alterations in glucose-fed rats. Part of the beneficial effects of SSR240612 appears to be associated with the normalization of B_1R gene and protein expression which is dependent on the oxidative stress.

Author Contributions

Conceived and designed the experiments: JPD PC RC. Performed the experiments: JPD ST JS. Analyzed the data: JPD ST JS. Contributed reagents/materials/analysis tools: PC. Wrote the paper: JPD RC.

References

1. Dias JP, Ismael MA, Pilon M, de Champlain J, Ferrari B, et al. (2007) The kinin B1 receptor antagonist SSR240612 reverses tactile and cold allodynia in an experimental rat model of insulin resistance. Br J Pharmacol 152: 280–287.
2. Lungu C, Dias JP, Franca CE, Ongali B, Regoli D, et al. (2007) Involvement of kinin B1 receptor and oxidative stress in sensory abnormalities and arterial hypertension in an experimental rat model of insulin resistance. Neuropeptides 41: 375–387.
3. Ismael MA, Talbot S, Carbonneau CL, Beausejour CM, Couture R (2008) Blockade of sensory abnormalities and kinin B(1) receptor expression by N-acetyl-L-cysteine and ramipril in a rat model of insulin resistance. Eur J Pharmacol 589: 66–72.
4. Marceau F, Sabourin T, Houle S, Fortin JP, Petitclerc E, et al. (2002) Kinin receptors: functional aspects. Int Immunol 2: 1729–1739.
5. Couture R, Girolami JP (2004) Putative roles of kinin receptors in the therapeutic effects of angiotensin 1-converting enzyme inhibitors in diabetes mellitus. Eur J Pharmacol 500: 467–485.
6. Regoli D, Nsa AS, Rizzi A, Gobeil FJ (1998) Bradykinin receptors and their antagonists. Eur J Pharmacol 348: 1–10.
7. El Midaoui A, Ongali B, Petcu M, Rodi D, de Champlain J, et al. (2005) Increases of spinal kinin receptor binding sites in two rat models of insulin resistance. Peptides 26: 1323–1330.
8. El Midaoui A, Wu R, de Champlain J (2002) Prevention of hypertension, hyperglycemia and vascular oxidative stress by aspirin treatment in chronically glucose-fed rats. J Hypertens 20: 1407–1412.
9. El Midaoui A, de Champlain J (2005) Effects of glucose and insulin on the development of oxidative stress and hypertension in animal models of type 1 and type 2 diabetes. J Hypertens 23: 581–588.
10. El Midaoui A, de Champlain J (2002) Prevention of hypertension, insulin resistance, and oxidative stress by alpha-lipoic acid. Hypertension 39: 303–307.
11. Campos MM, Leal PC, Yunes RA, Calixto JB (2006) Non-peptide antagonists for kinin B1 receptors: new insights into their therapeutic potential for the management of inflammation and pain. Trends Pharmacol Sci 27: 646–651.
12. Gougat J, Ferrari B, Sarran L, Planchenault C, Poncelet M, et al. (2004) SSR240612 [(2R)-2-[((3R)-3-(1,3-benzodioxol-5-yl)-3-[[(6-methoxy-2-naphthyl)-sulfonyl]amino]propanoyl)amino]-3-(4-[[2R,6S)-2,6-dimethylpiperidinyl]-methyl]pheny l)-N-isopropyl-N-methylpropanamide hydrochloride], a new nonpeptide antagonist of the bradykinin B1 receptor: biochemical and pharmacological characterization. J Pharmacol Exp Ther 309: 661–669.
13. Mori MA, Araujo RC, Reis FC, Sgai DG, Fonseca RG, et al. (2008) Kinin B1 receptor deficiency leads to leptin hypersensitivity and resistance to obesity. Diabetes 57: 1491–1500.
14. Matthews DR, Hosker JP, Rudenski AS, Naylor BA, Treacher DF, et al. (1985) Homeostasis model assessment: insulin resistance and beta-cell function from fasting plasma glucose and insulin concentrations in man. Diabetologia 28: 412–419.
15. Munzel T, Sayegh H, Freeman BA, Tarpey MM, Harrison DG (1995) Evidence for enhanced vascular superoxide anion production in nitrate tolerance. A novel mechanism underlying tolerance and cross-tolerance. J Clin Invest 95: 187–194.
16. Heitzer T, Wenzel U, Hink U, Krollner D, Skatchkov M, et al. (1999) Increased NAD(P)H oxidase-mediated superoxide production in renovascular hypertension: evidence for an involvement of protein kinase C. Kidney Int 55: 252–260.
17. Loomis ED, Sullivan JC, Osmond DA, Pollock DM, Pollock JS (2005) Endothelin mediates superoxide production and vasoconstriction through activation of NADPH oxidase and uncoupled nitric-oxide synthase in the rat aorta. J Pharmacol Exp Ther 315: 1058–1064.
18. Tawfik HE, Cena J, Schulz R, Kaufman S (2008) Role of oxidative stress in multiparity-induced endothelial dysfunction. Am J Physiol Heart Circ Physio 295: H1736–H1742.
19. Drapeau G, Audet R, Levesque L, Godin D, Marceau F (1993) Development and in vivo evaluation of metabolically resistant antagonists of B1 receptors for kinins. J Pharmacol Exp Ther 266: 192–199.
20. Miller FJ, Jr., Gutterman DD, Rios CD, Heistad DD, Davidson BL (1998) Superoxide production in vascular smooth muscle contributes to oxidative stress and impaired relaxation in atherosclerosis. Circ Res 82: 1298–1305.
21. Aoki S, Su Q, Li H, Nishikawa K, Ayukawa K, et al. (2002) Identification of an axotomy-induced glycosylated protein, AIGP1, possibly involved in cell death triggered by endoplasmic reticulum-Golgi stress. J Neurosci 22: 10751–10760.
22. Wada R, Tifft CJ, Proia RL (2000) Microglial activation precedes acute neurodegeneration in Sandhoff disease and is suppressed by bone marrow transplantation. Proc Natl Acad Sci U S A 97: 10954–10959.
23. Livak KJ, Schmittgen TD (2001) Analysis of relative gene expression data using real-time quantitative PCR and the 2(-Delta Delta C(T)) Method. Methods 25: 402–408.

24. Cloutier F, de Sousa BH, Ongali B, Couture R (2002) Pharmacologic and autoradiographic evidence for an up-regulation of kinin B(2) receptors in the spinal cord of spontaneously hypertensive rats. Br J Pharmacol 135: 1641–1654.
25. Nazarali AJ, Gutkind JS, Saavedra JM (1989) Calibration of 125I-polymer standards with 125I-brain paste standards for use in quantitative receptor autoradiography. J Neurosci Methods 30: 247–253.
26. Anand-Srivastava MB, de Champlain J, Thibault C (1993) DOCA-salt hypertensive rat hearts exhibit altered expression of G-proteins. Am J Hypertens 6: 72–75.
27. Pesquero JB, Araujo RC, Heppenstall PA, Stucky CL, Silva JA, Jr., et al. (2000) Hypoalgesia and altered inflammatory responses in mice lacking kinin B1 receptors. Proc Natl Acad Sci U S A 97: 8140–8145.
28. Calixto JB, Medeiros R, Fernandes ES, Ferreira J, Cabrini DA, et al. (2004) Kinin B1 receptors: key G-protein-coupled receptors and their role in inflammatory and painful processes. Br J Pharmacol 143: 803–818.
29. Gabra BH, Berthiaume N, Sirois P, Nantel F, Battistini B (2006) The kinin system mediates hyperalgesia through the inducible bradykinin B1 receptor subtype: evidence in various experimental animal models of type 1 and type 2 diabetic neuropathy. Biol Chem 387: 127–143.
30. Quintao NL, Passos GF, Medeiros R, Paszcuk AF, Motta FL, et al. (2008) Neuropathic pain-like behavior after brachial plexus avulsion in mice: the relevance of kinin B1 and B2 receptors. J Neurosci 28: 2856–2863.
31. Hall CE, Hall O (1966) Comparative ability of certain sugars and honey to enhance saline polydipsia and salt hypertension. Proc Soc Exp Biol Med 122: 362–365.
32. Hwang IS, Ho H, Hoffman BB, Reaven GM (1987) Fructose-induced insulin resistance and hypertension in rats. Hypertension 10: 512–516.
33. Vasdev S, Longerich L, Gill V (2004) Prevention of fructose-induced hypertension by dietary vitamins. Clin Biochem 37: 1–9.
34. Cavarape A, Feletto F, Mercuri F, Quagliaro L, Daman G, et al. (2001) High-fructose diet decreases catalase mRNA levels in rat tissues. J Endocrinol Invest 24: 838–845.
35. Nyby MD, Abedi K, Smutko V, Eslami P, Tuck ML (2007) Vascular Angiotensin type 1 receptor expression is associated with vascular dysfunction, oxidative stress and inflammation in fructose-fed rats. Hypertens Res 30: 451–457.
36. Thirunavukkarasu V, Nitha Nandhini AT, Anuradha CV (2004) Effect of alpha-lipoic acid on lipid profile in rats fed a high-fructose diet. Exp Diabesity Res 5: 195–200.
37. Vasdev S, Ford CA, Longerich L, Parai S, Gadag V, et al. (1999) Aldehyde induced hypertension in rats: prevention by N-acetyl cysteine. Artery 23: 10–36.
38. Pop-Busui R, Sima A, Stevens M (2006) Diabetic neuropathy and oxidative stress. Diabetes Metab Res Rev 22: 257–273.
39. Rodriguez AI, Pereira-Flores K, Hernandez-Salinas R, Boric MP, Velarde V (2006) High glucose increases B1-kinin receptor expression and signaling in endothelial cells. Biochem Biophys Res Commun 345: 652–659.
40. Shoelson SE, Lee J, Goldfine AB (2006) Inflammation and insulin resistance. J Clin Invest 116: 1793–1801.
41. Csiszar A, Wang M, Lakatta EG, Ungvari Z (2008) Inflammation and endothelial dysfunction during aging: role of NF-kappaB. J Appl Physiol 105: 1333–1341.
42. Paravicini TM, Touyz RM (2008) NADPH oxidases, reactive oxygen species, and hypertension: clinical implications and therapeutic possibilities. Diabetes Care Suppl 2: S170–80. Review.
43. Tong X, Schroder K (2009) NADPH oxidases are responsible for the failure of nitric oxide to inhibit migration of smooth muscle cells exposed to high glucose. Free Radic Biol Med 47: 1578–1583.
44. Gao L, Mann GE (2009) Vascular NAD(P)H oxidase activation in diabetes: a double-edged sword in redox signalling. Cardiovasc Res 82: 9–20.
45. Li Y, Descorbeth M, Anand-Srivastava MB (2008) Role of oxidative stress in high glucose-induced decreased expression of Gialpha proteins and adenylyl cyclase signaling in vascular smooth muscle cells. Am J Physiol Heart Circ Physiol 294(6): H2845–54.
46. San Martín A, Du P, Dikalova A, Lassègue B, Aleman M, et al. (2007) Reactive oxygen species-selective regulation of aortic inflammatory gene expression in Type 2 diabetes. Am J Physiol Heart Circ Physiol 5: H2073–82.
47. Clerch LB, Massaro D (1993) Tolerance of rats to hyperoxia. Lung antioxidant enzyme gene expression. J Clin Invest 91: 499–508.
48. Ceriello A, Dello RP, Amstad P, Cerutti P (1996) High glucose induces antioxidant enzymes in human endothelial cells in culture. Evidence linking hyperglycemia and oxidative stress. Diabetes 45: 471–477.
49. Sharpe PC, Liu WH, Yue KK, McMaster D, Catherwood MA, et al. (1998) Glucose-induced oxidative stress in vascular contractile cells: comparison of aortic smooth muscle cells and retinal pericytes. Diabetes 47: 801–809.
50. Majithiya JB, Balaraman RJ (2005) Time-dependent changes in antioxidant enzymes and vascular reactivity of aorta in streptozotocin-induced diabetic rats treated with curcumin. J Cardiovasc Pharmacol 46(5): 697–705.
51. Fernandes L, Ceravolo GS, Fortes ZB, Tostes R, Santos RA, et al. (2006) Modulation of kinin B1 receptor expression by endogenous angiotensin II in hypertensive rats. Regul Pept 136: 92–97.
52. Ceravolo GS, Fernandes L, Munhoz CD, Fernandes DC, Tostes RC, et al. (2007) Angiotensin II chronic infusion induces B1 receptor expression in aorta of rats. Hypertension 50: 756–761.
53. Petcu M, Ongali B, El Midaoui A, de Champlain J, Couture R (2005) Effects of alpha-lipoic acid on kinin B1 and B2 receptor binding sites in the spinal cord of chronically angiotensin-treated rats. Peptides 26: 1331–1338.
54. Kintsurashvili E, Duka I, Gavras I, Johns C, Farmakiotis D, et al. (2001) Effects of ANG II on bradykinin receptor gene expression in cardiomyocytes and vascular smooth muscle cells. Am J Physiol Heart Circ Physiol 281: H1778–H1783.
55. Rajagopalan S, Kurz S, Munzel T, Tarpey M, Freeman BA, et al. (1996) Angiotensin II-mediated hypertension in the rat increases vascular superoxide production via membrane NADH/NADPH oxidase activation. Contribution to alterations of vasomotor tone. J Clin Invest 97: 1916–1923.
56. Mehta PK, Griendling KK (2007) Angiotensin II cell signaling: physiological and pathological effects in the cardiovascular system. Am J Physiol Cell Physiol 292: C82–C97.
57. Leeb-Lundberg LM, Marceau F, Muller-Esterl W, Pettibone DJ, Zuraw BL (2005) International union of pharmacology. XLV. Classification of the kinin receptor family: from molecular mechanisms to pathophysiological consequences. Pharmacol Rev 57: 27–77.
58. De Brito GH, Carayon P, Ferrari B, Couture R (2010) Contribution of the central dopaminergic system in the anti-hypertensive effect of kinin B1 receptor antagonists in two rat models of hypertension. Neuropeptides 44: 191–198.
59. Dias JP, Étude du rôle des kinines dans les neuropathies et l'hypertension artérielle chez le rat diabétique, Thesis-Université Montreal,cote W4U58 2008 v.020 ex., 2.
60. Buleon M, Allard J, Jaafar A, Praddaude F, Dickson Z, et al. (2008) Pharmacological blockade of B2-kinin receptor reduces renal protective effect of angiotensin-converting enzyme inhibition in db/db mice model. Am J Physiol Renal Physiol 294: F1249–F1256.
61. Chao J, Yin H, Gao L, Hagiwara M, Shen B, et al. (2008) Tissue kallikrein elicits cardioprotection by direct kinin B2 receptor activation independent of kinin formation. Hypertension 52: 715–720.
62. Chao J, Shen B, Gao L, Xia CF, Bledsoe G, et al. (2010) Tissue kallikrein in cardiovascular, cerebrovascular and renal diseases and skin wound healing. Biol Chem 391: 345–355.
63. Methner C, Donat U, Felix SB, Krieg T (2009) Cardioprotection of bradykinin at reperfusion involves transactivation of the epidermal growth factor receptor via matrix metalloproteinase-8. Acta Physiol (Oxf) 197: 265–271.
64. Kakoki M, Sullivan KA, Backus C, Hayes JM, Oh SS, et al. (2010) Lack of both bradykinin B1 and B2 receptors enhances nephropathy, neuropathy, and bone mineral loss in Akita diabetic mice. Proc Natl Acad Sci U S A 107: 10190–10195.
65. Savvatis K, Westermann D, Schultheiss HP, Tschope C (2010) Kinins in cardiac inflammation and regeneration: insights from ischemic and diabetic cardiomyopathy. Neuropeptides 44: 119–125.
66. Messadi-Laribi E, Griol-Charhbili V, Gaies E, Vincent MP, Heudes D, et al. (2008) Cardioprotection and kallikrein-kinin system in acute myocardial ischaemia in mice. Clin Exp Pharmacol Physiol 35: 489–493.
67. Kakoki M, Smithies O (2009) The kallikrein-kinin system in health and in diseases of the kidney. Kidney Int 75: 1019–1030.
68. Xu J, Carretero OA, Sun Y, Shesely EG, Rhaleb NE, et al. (2005) Role of the B1 kinin receptor in the regulation of cardiac function and remodeling after myocardial infarction. Hypertension 45: 747–753.
69. Lagneux C, Bader M, Pesquero JB, Demenge P, Ribuot C (2002) Detrimental implication of B1 receptors in myocardial ischemia: evidence from pharmacological blockade and gene knockout mice. Int Immunopharmacol 2: 815–822.
70. Duka A, Kintsurashvili E, Duka I, Ona D, Hopkins TA, et al. (2008) Angiotensin-converting enzyme inhibition after experimental myocardial infarct: role of the kinin B1 and B2 receptors. Hypertension 51: 1352–1357.
71. Wang PH, Cenedeze MA, Campanholle G, Malheiros DM, Torres HA, et al. (2009) Deletion of bradykinin B1 receptor reduces renal fibrosis. Int Immunopharmacol 9: 653–657. S1567-5769.
72. Kakoki M, Takahashi N, Jennette JC, Smithies O (2004) Diabetic nephropathy is markedly enhanced in mice lacking the bradykinin B2 receptor. Proc Natl Acad Sci U S A 101: 13302–13305.
73. Kakoki M, Kizer CM, Yi X, Takahashi N, Kim HS, et al. (2006) Senescence-associated phenotypes in Akita diabetic mice are enhanced by absence of bradykinin B2 receptors. J Clin Invest 116: 1302–1309.
74. Duka I, Kintsurashvili E, Gavras I, Johns C, Bresnahan M, et al. (2001) Vasoactive potential of the B(1) bradykinin receptor in normotension and hypertension. Circ Res 88: 275–281.
75. Seguin T, Buleon M, Destrube M, Ranera MT, Couture R, et al. (2008) Hemodynamic and renal involvement of B1 and B2 kinin receptors during the acute phase of endotoxin shock in mice. Int Immunopharmacol 8: 217–221.
76. Rodrigues ES, Martin RP, Felipe SA, Bader M, Oliveira SM, et al. (2009) Cross talk between kinin and angiotensin II receptors in mouse abdominal aorta. Biol Chem 390: 907–913.
77. Rodrigues ES, Martin RP, Pesquero JB, Shimuta SI (2010) Lack of kinin receptors affected ACE expression in mice abdominal aorta. Basic and Clinical Pharmacology and Toxicology 107(suppl.1, paper No: 2813.
78. Shariat-Madar Z, Mahdi F, Warnock M, Homeister JW, Srikanth S, et al. (2006) Bradykinin B2 receptor knockout mice are protected from thrombosis by increased nitric oxide and prostacyclin. Blood 108: 192–199.